Effect of subtherapeutic and therapeutic sulfamethazine concentrations on transcribed genes and translated proteins involved in Microbacterium sp. C448 resistance and degradation

Laurianne Paris, Marion Devers-Lamrani, Muriel Joly, Didier Viala, Marie de Antonio, Bruno Pereira, Nadine Rouard, Pascale Besse-Hoggan, Michel Hébraud, Edward Topp, et al.

Effect of subtherapeutic and therapeutic sulfamethazine concentrations on transcribed genes and translated proteins involved in *Microbacterium* sp. C448 resistance and degradation

Laurianne Paris[1,2,*], Marion Devers-Lamrani[3], Muriel Joly[1,2], Didier Viala[4], Marie De Antonio[5], Bruno Pereira[5], Nadine Rouard[3], Pascale Besse-Hoggan[2], Michel Hébraud[4,6], Edward Topp[7,8], Fabrice Martin-Laurent[3], Isabelle Batisson[1]

1 Université Clermont Auvergne, CNRS, LMGE, F-63000 Clermont-Ferrand, France. 2 Université Clermont Auvergne, CNRS, ICCF, F-63000 Clermont-Ferrand, France. 3 Institut Agro, INRAE, Université de Bourgogne, Université de Bourgogne Franche-Comté, Agroécologie, F-21000 Dijon, France. 4 INRAE Site de Theix, Plate-forme d'exploration du métabolisme, F-63122 Saint-Genès Champanelle, France. 5 Biostatistics Unit (DRCI), Clermont-Ferrand University Hospital, F-63000 Clermont-Ferrand, France. 6 Université Clermont Auvergne, INRAE, UMR MEDiS, F-63122 Saint-Genès Champanelle, France. 7 London Research and Development Centre, Agriculture and Agri-Food Canada, London, ON N5V 4T3, Canada. 8 Department of Biology, University of Western Ontario, London, ON N6A 3K7.

*Corresponding author: Laboratoire Microorganismes: Génome et Environnement, 1 Impasse Amélie Murat, TSA 60026, CS 60026, 63178 Aubière Cedex, France. E-mail address: laurianne.paris@uca.fr

Abstract

Microbacterium sp. C448, isolated from a soil regularly exposed to sulfamethazine (SMZ), can use various sulphonamide antibiotics as the sole carbon source for growth. The basis for the regulation of genes encoding the sulphonamide metabolism pathway, the dihydropteroate synthase sulphonamide target (*folP*), and the sulphonamide resistance (*sul1*) genes, is unknown in this organism. In the present study, the response of the transcriptome and proteome of *Microbacterium* sp. C448 following exposure to subtherapeutic (33 µM) or therapeutic (832 µM) SMZ concentrations was evaluated.

Therapeutic concentration induced the highest *sad* expression and Sad production, consistent with the activity of SMZ degradation observed *in cellulo*. Following complete SMZ degradation, Sad production tended to return to the basal level observed prior to SMZ exposure. Transcriptomic and proteomic kinetics were concomitant for the resistance genes and proteins. The abundance of Sul1 protein, 100-fold more abundant than FolP protein, did not change in response to SMZ exposure. Moreover, non-targeted analyses highlighted the increase of a deaminase RidA and a putative sulphate exporter expression and production. These two novel factors involved in the 4-aminophenol metabolite degradation and the export of sulphate residues formed during SMZ degradation, respectively, provided new insights into *Microbacterium* sp. C448 SMZ detoxification process.

Keywords: Sulphonamide antibiotic, *sad* gene, dihydropteroate synthase, omic approaches, deaminase RidA, sulphate exporter

Introduction

In commercial food-animal production, antibiotics are used therapeutically, for prophylaxis and, in some jurisdictions, for growth promotion (van Boeckel *et al.* 2017). Following ingestion by farm animals, some antibiotics are excreted intact, and thus animal wastes can represent a major source of antibiotic entry into the environment (Feng *et al.* 2017; Deng *et al.* 2018; Mulla *et al.* 2021). Amendment of crop production systems with manures can lead to the contamination of soil, surface and ground-waters with antibiotics, representing a potential threat to human and environmental health (Spielmeyer *et al.* 2017; Spielmeyer 2018; Ben *et al.* 2019; National Academy of Pharmacy 2019; Duan *et al.* 2022).

In France, the sulphonamides are the second most widely used class of antibiotics used in food animal production, representing 19.8% or 73.6 tonnes sold in 2021. Although their use has decreased since the beginning of the 2000s (Anses 2022), their presence in the environment represents a potential risk for ecosystems because of the possible selection and dissemination of sulphonamide-

resistance genes and resistant bacteria. Sulphonamides inhibit the dihydropteroate synthase (DHPS, EC 2.5.1.15; encoded by the *fol*P gene), a key enzyme involved in the folate biosynthetic pathway in bacteria and some unicellular eukaryotes, by competition with the substrate *p*-amino benzoic acid (Capasso and Supuran 2014). Folate is a precursor for the biosynthesis of tetrahydrofolate, a key coenzyme required for the synthesis of some nucleotides and amino acids. Sulphonamides are bacteriostatic to many Gram-negative and Gram-positive bacteria (Connor 1998). The bacterial resistance is mainly due to mutations in the *folP* gene or the acquisition of alternative genes (*sul1*, *sul2*, and *sul3*) encoding DHPS proteins that do not interact with the sulphonamide antibiotics (Sköld 2000; Perreten and Boerlin 2003; Martin-Laurent *et al.* 2014; Zhou *et al.* 2021).

In the environment, the removal of sulphonamides can result from chemical or biological degradation (Chen and Xie 2018; Mulla *et al.* 2021; Hu *et al.* 2022) and is dependent on a variety of factors such as the sulphonamide concentration, and key rate-controlling parameters such as temperature and pH (Cao *et al.* 2019; Chen *et al.* 2019). Different biodegradation pathways have been described for various sulphonamide-degrading bacteria isolated from activated sludge, wastewater or contaminated soil (Chen and Xie 2018; Nunes *et al.* 2020; Perri, Kolvenbach and Corvini 2020). Notably, some *Microbacterium* spp. strains isolated from manured soil, sediment or activated sludge, use sulphonamides as the sole carbon source (Bouju *et al.* 2012; Tappe *et al.* 2013; Topp *et al.* 2013; Kim *et al.* 2019b). Sulphonamide biodegradation by *Microbacterium* spp. requires a gene cluster encoding three proteins; two flavin-dependent monooxygenases, SadA and SadB, possessing an acyl-CoA dehydrogenase domain, and the flavin reductase, SadC (Ricken *et al.* 2017). The latter reduces the flavin mononucleotide (FMN) cofactor required for the activity of the two monooxygenases. The role of the Sad component system in sulphonamide degradation has only been demonstrated *in vitro* using purified enzymes (Ricken *et al.* 2017; Kim *et al.* 2019b). Sulfamethazine (SMZ, also called sulfadimidine), which can reach maximum concentration of 20-25 mg per kg manure or soil (Cycoń *et al.* 2019), is transformed by SadA into 4-aminophenol (4AP), the dead-end product 2-amino-4,6-dimethylpyrimidine (ADMP) in stoichiometric amounts and sulphur dioxide (Ricken *et al.* 2017) (Fig.

S1). The 4-aminophenol is then transformed by SadB to 1,2,4-trihydroxybenzene which is ultimately mineralized. This degradation pathway is conserved in the Micrococcales order (Kim *et al.* 2019b).

In addition to carrying the *sad* gene cluster, *Microbacterium* sp. strain C448 carries the *sul1* gene (Martin-Laurent *et al.* 2014). The relative significance and interplay of the sulphonamide biodegradation pathway and the *sul1* resistance gene in the organism's ability to tolerate and then metabolize the sulphonamides remains unclear.

In the present study, transcriptomic and proteomic approaches were used to evaluate the expression levels of the *sad*, *folP* and *sul1* genes, and the abundance of their corresponding proteins. Changes in response to exposure to low subtherapeutic-relevant concentrations and to higher therapeutically-relevant concentrations of SMZ were evaluated. We hypothesized that at low subtherapeutic concentration, *sul1* would not be required to permit biodegradation of the drug whereas at high concentration it would. Time-series transcript- and protein-profiles were analysed and compared to a non-exposed *Microbacterium* culture.

Materials and Methods

Strain and medium

Microbacterium sp. strain C448 was isolated from field soil on the Agriculture and Agri-Food Canada research farm in London (Ontario) that was intentionally treated annually for several years with 10 mg SMZ per kg soil. Descriptions of the field, methods for primary isolation, identification and characterization of the isolate are available in Topp *et al.* (2013) and Martin-Laurent *et al.* (2014). The bacterium was cultured in a defined medium (DM) containing glucose (0.5% w/v), amino acids (0.1 g/L of Cys, Trp, Leu, Ile, Val and Met; 0.2 g/L of Arg, and 0.6 g/L of His, Glu), and salts, vitamins and trace elements prepared as described in Amezaga *et al.* (1995). Sulfamethazine sodium salt was purchased from Sigma Aldrich (Saint-Quentin-Fallavier, France; purity ≥ 98%). A stock solution (333 mM, 100 g/L) was prepared in water, sterilized by filtration (0.2 µm) and stored at -20 °C until used.

Culture conditions and sample preparation

Transcriptomic and proteomic analyses were performed after cultivation of *Microbacterium* sp. C448 strain in DM medium at 28 °C with agitation (150 rpm). The growth was monitored by measuring absorbance at 600 nm (OD_{600}). The bacterial cells were collected at the mid-exponential growth phase by centrifugation (5 min, 5,000 x *g*) and washed twice in DM medium. For each experiment, forty Erlenmeyer flasks (50 and 500 mL) containing respectively 20 mL (transcriptomic) or 180 mL (proteomic) of DM medium, were inoculated with the washed cells at an OD_{600} of 0.4. The flasks were supplemented with 33 µM of SMZ sodium salt (corresponding to 10 mg/L, low concentration, LC), 832 µM of SMZ sodium salt (corresponding to 250 mg/L, high concentration, HC) or unsupplemented (Control, no SMZ) before being incubated at 28 °C with agitation (150 rpm) in the dark. A set of four flasks were sacrificed for each concentration immediately after inoculation (T0), at an early SMZ degradation rate (0.6 h and 1 h post-inoculation (pi)), at an advanced SMZ degradation rate (5 h pi) and after complete SMZ degradation (9 h and 24 h pi) for the transcriptomic and proteomic analyses, respectively. For each sacrificed flask, OD_{600} was measured, and 1 mL of culture was centrifuged (3 min, 10,000 x *g*) to quantify SMZ and ADMP in the supernatant by HPLC. The remaining culture was used for the RNA or protein extractions.

SMZ and ADMP quantification by HPLC

The concentrations of SMZ and its dead-end transformation product ADMP were determined by HPLC on an Agilent 1100 apparatus (Agilent Technologies, Courtaboeuf, France) equipped with a reverse-phase column (C18 Zorbax Eclipse Plus column, 75 mm × 4.6 mm, 3.5 µm) at 22 °C and a diode array detector set at λ = 260 nm (SMZ, retention time = 9.3 min) and 298 nm (ADMP, retention time = 1.1 min). The mobile phase was composed of aqueous H_3PO_4 (0.01% v/v, pH = 2.9) (A) and acetonitrile (B) at a flow rate of 1 mL/min. Gradient (linear): 0–5 min: 2% B; 5–8 min: 2–30% B; 8–10 min: 30–90% B; 10–11 min: 90–100% B; 11–13 min: 100–2% B. Injection volume: 5 µL. Each sample was analysed twice (technical duplicates). SMZ (Sigma Aldrich, purity > 99%) and ADMP (Alfa Aesar, Thermo Fischer

Scientific, Walthman, MA, USA; purity 98%) were used as analytical standards. Concentrated solutions (100 µM and 1 mM, respectively) were prepared in distilled water and diluted to obtain known concentration solutions in order to have a six-point standard curve for each compound at each concentration range (0-100 µM and 0-1 mM, respectively).

Transcriptomic experiment

RNA extraction and sequencing

RNeasy® Protect Bacteria Mini Kit (QIAGEN, Germantown, MD, USA) was used for the RNA extraction, according to the manufacturer recommendations. Briefly, 2.5 mL of cell suspension were mixed with 5 mL of bacterial RNAprotect™ Reagent (QIAGEN) and incubated for 5 min at room temperature before centrifugation (5,000 g, 10 min). The cells were lysed using lysozyme, proteinase K digestion and mechanical disruption by mixing cells with 0.2 g of acid washed beads (212-300 µm size, Sigma Aldrich) in a FastPrep-24™ classic apparatus (twice 30 s at 6 m/s, MP Biomedicals, Illkirch, France). RNA was purified on a column treated with DNAse. The quality and the quantity of extracted RNA were estimated using the RNA 6000 Nano LabChip® Kit and the 2100 Bioanalyzer following the manufacturer recommendations (Agilent Technologies). For each sample, more than 500 ng of total RNA were sent to GENEWIZ® (Azenta Life Science, Leipzig, Germany) which performed the rRNA depletion, the cDNA synthesis, and the adapter ligation. The obtained library was sequenced in an Illumina® NovaSeq™ 6000 apparatus (2 x 150 bp paired-end reads, Illumina, San Diego, CA, USA). More than 18 Mreads were generated per sample with a quality score ≥ 36.

Bioinformatic analysis and data treatment

The reads were first quality-filtered and trimmed using the wrapper script trim galore (v0.6.4) using cutadapt (v2. 6) to trim the reads (Babraham Bioinformatics) (Martin 2011). The reads were then aligned to the genome of *Microbacterium* sp. C448 using hisat2 (v2.2.1) (Kim *et al.* 2019a), and counted

using featureCounts (v2.0.1) (Liao *et al.* 2014). The differences of normalized gene expressions between control and SMZ-treated conditions were highlighted using DESeq2 (Love *et al.* 2014). The RNA counting was standardised between samples using Moose2 (polynoMial nOrmalization Of RNA-SEq data), allowing to normalize FPKM (Fragments per kilo-base per million) or RPKM (reads per kilobase per million) values from multiple samples to correct for non-linear artifacts, introduced by the library construction and/or sequencing process (Annergren and Larsson 2016).

Data availability

The sequencing data have been submitted to the Sequence Read Archive (SRA, NIH, NCBI), with the project number PRJNA860753.

Proteomic experiment

Protein extraction

The proteins were extracted according to the cell fractionation method described by Esbelin *et al.* (2018) and Santos and Hébraud (2021) with some modifications. For each flask, 180 mL of bacterial culture was centrifuged (5 min, 4,800 x *g*) and the pellet was washed twice in 30 mL of Phosphate Buffered Saline (pH 7.4). Washed pellet was suspended in 4 mL of Tris-EDTA (20 mM Tris; 5 mM, pH 7). Bacterial cells were broken by three passages through a French-press cell disrupter (One Shot Cell Disruptor, Constant Systems Ltd., Daventury, United Kingdom) set at a pressure of 2.6 kbar. After centrifugation (13,000 x *g*, 15 min, 4 °C), the supernatants, mainly containing the soluble proteins (cytosol) but also some membrane pieces and their integrated proteins, were recovered and conserved at -20 °C in 50 mL Protein LoBind® Tubes (Eppendorf, Hamburg, Germany). The pellets, containing the proteins of the cell envelope, were washed twice with 5 mL of Tris 40 mM (pH 8.5), suspended in 200 to 600 µL of Tris 25 mM (pH 6.8), depending to the pellet viscosity, and conserved at -20 °C in 1.5 ml Protein LoBind® Tubes (Eppendorf). The quantification of the proteins was performed in triplicate

following the protocol of the Pierce™ Coomassie (Bradford) Protein Assay Kit (Thermo Fischer Scientific, Waltham, MA, USA). The absorbance was read at 596 nm using a microplate reader (Thermo Multiskan™ FC, Thermo Fischer Scientific). Short electrophoresis was performed on 12% SDS-polyacrylamide electrophoresis gels to concentrate 10 µg of proteins per sample in the first millimetres of the resolution gel. The concentrated protein band was manually excised with a sterile scalpel blade and washed, reduced, alkylated and digested by trypsin treatment before the nano-LC-MS/MS analysis as detailed in Esbelin *et al.* (2018) and Santos and Hébraud (2021), with some details. The reduction of disulphide bonds was achieved in 10 mM dithiothreitol prepared in 50 mM ammonium bicarbonate buffer and the incubation was carried out for 30 min at 56 °C. The alkylation of proteins was carried out with 55 mM iodoacetamide prepared in 50 mM ammonium bicarbonate buffer for 30 min in darkness. Finally, bands were dehydrated with 100% acetonitrile for 10 min and the liquid was discarded. The proteins were hydrolysed in 600 ng of trypsin in a 50 mM ammonium bicarbonate buffer for 5 h at 37 °C, ensuring that bands were always in liquid by addition of buffer. Peptides were extracted for 15 min in ultrasound bath with 40 µL of acetonitrile/trifluoroacetic acid (TFA) (99.9/0.1 v/v). The supernatants were dry concentrated with a SpeedVac® concentrator (Thermo Savant SPD 1010, Thermo Fischer Scientific) for 2 h. The volume was adjusted to 40 µL with a solution of Water/Acetonitrile/TFA (95/5/0.05 v/v/v). After 10 min of ultrasonic bath (VWR® USC, Ultrasonic cleaner USC 600TH, Avantor®, Radnor, PA, USA), the entire supernatant was transferred to a glass HPLC vial prior to LC MS/MS analysis.

Quantification of proteins by nano-LC-MS/MS and bioinformatic analyses

Peptide mixtures were randomised before being analysed by nano-LC-MS/MS using the RSLC nano Ultimate™ 3000 (Thermo Fischer Scientific) coupled to the Q Exactive HF-X Hybrid Quadrupole-Orbitrap mass spectrometer (MS) (Thermo Fischer Scientific) with a nano-electrospray ion source. Initially, 1 µL of hydrolysate was preconcentrated and desalted at a flow rate of 30 µL/min on a C18 pre-column 5 cm length x 100 µm (Acclaim™ PepMap™ 100 C18, 5 µm, 100 Å nanoViper, Thermo Fisher

Scientific) equilibrated with TFA 0.05% in water. In a second step, the concentration column was switched online with a nanoflow analytical C18 column (Acclaim™ PepMap™ 100 - 75 µm inner diameter × 25 cm length; C18 - 3 µm – 100 Å, Thermo Fisher Scientific) equilibrated with a 95% solvent A (99.9% H_2O, 0.1% formic acid) flow at 300 nL/min. The peptides were then separated according to their hydrophobicity with a 55 min gradient of solvent B (99.9% acetonitrile, 0.1% formic acid) from 5 to 32%. For MS analysis, eluted peptides were electrosprayed in positive-ion mode at 1.6 kV through a nano-electrospray ion source heated to 250 °C. The mass spectrometer operated in data dependent mode: the parent ion was selected in the orbitrap cell (FTMS) at a resolution of 120,000 and each MS analysis was followed by 18 MS/MS with analysis of the MS/MS fragments at a resolution of 15,000.

For raw data processing, MS/MS ion search was carried out with Mascot v2.5.1 (http://www.matrixscience.com, Matrix Science) against the UniProt reference database of *Microbacterium* sp. C448 (*i.e.* ref_microb_spc448 20190711-3165 sequences) with the following parameters during the request: precursor mass tolerance of 10 ppm and fragment mass tolerance of 0.02 Da, a maximum of two missed cleavage sites of trypsin, carbamidomethylation, oxidation of Methionine and deamidation Asparagine and Glutamine set as variable modifications. Protein identification was validated when at least two peptides from one protein showed statistically significant identity above Mascot scores with a False Discovery Rate of 1%. Ion scores was -10 log(P), where *P* was the probability that the observed match was a random event. The Mascot score was respectively 14 with an adjusted *p*-value of 0.05 for supernatants and 34 with an adjusted *p*-value of 0.05 for pellets. The Progenesis® QI for proteomics v4.2 software (Nonlinear Dynamics©, Waters™, Milford, MA, USA) was used for the label-free protein quantitation analysis, with the same identification parameters as described above. All unique validated peptides of an identified protein were included, and the total cumulative abundance was calculated by summing the abundances of all peptides allocated to the respective protein. With the Progenesis® QI software, the proteomic LC-MS/MS data were statistically analysed using the “between subject design” and *p*-values were calculated by a repeated measures analysis of variance using the normalized abundances across all

runs. Obtained data were expressed in arbitrary unit (AU) corresponding to the areas under the peaks obtained by nano LC-MS/MS normalized by the number of cells.

~~The SMZ degradation genes and proteins *sadA*/SadA (ORF 2030/UniProt number W0Z5L8), *sadB*/SadB (ORF 2028/W0Z833) and *sadC*/SadC (ORF 2026/W0Z7H5), and the SMZ target genes and proteins: *folP*/FolP (ORF 1952/W0Z6Y9) and *sul1*/Sul1 (ORF 2696/W0Z673) were specifically studied.~~

Statistical analyses

The statistical analyses were performed using R software (The R Foundation). For the transcriptomic data, the package DESeq2 was used. It is based on the use of negative binomial generalized linear models on un-normalized counts. It allows to determine for each open reading frame (ORF) and at each sampling time whether its level of expression is different between the control and LC or HC condition. Since transcriptional regulation is a short-term response and mRNAs are labile, ORF presenting an expression level different by at least by a factor of two in the presence of SMZ in the medium, and a Benjamini-Hochberg adjusted *p*-value (Benjamini and Hochberg 1995) inferior to 0.001, was considered as having a significant differential gene expression level compared to the SMZ-free control (Love *et al.* 2014).

For the proteomic data, the assumptions of normality were assessed using several tests (Shapiro-Wilk, Kolmogorov-Smirnov, Jarque-Bera and D'Agostino tests). Box-Cox transformation was applied to achieve normality when appropriate and an ANOVA test followed by Tukey post-hoc were applied with a α risk of 0.05. For the analysis of resistance markers, which turned out to be non-parametric even with the transformation, a Kruskal-Wallis test followed by Dunn's test were applied. The fold-change was calculated at the three sampling time, comparing LC and HC SMZ concentrations *versus* control. For proteomic data, the significant comparisons with a minimum fold-change of $\pm$ 1.5 were considered as relevant for the *a priori* analyses on Sad and DHPS proteins, and of 2.0 concerning the analyses on resistance markers without *a priori* consideration.

Results and Discussion

Kinetics of SMZ degradation by *Microbacterium* sp. strain C448

The degradation of SMZ by *Microbacterium* sp. C488 started immediately following the addition of 33 µM SMZ, and followed a typical single first-order kinetics (Fig. 1A and 1B). The degradation rate was very rapid with similar rate constants in the transcriptomic ($k = 0.96\ h^{-1}$ $r^2 = 0.9753$) and proteomic ($k = 1.1\ h^{-1}$ $r^2 = 1$) experiments. The SMZ was completely degraded within 5 h of incubation. Under the HC condition (Fig. 1C and 1D), the degradation kinetics were rather different between both experiments. The transcriptomic experiments showed a disappearance of 600 µM (72%) of the initial SMZ concentration at 5 h pi, and complete degradation at 9 h pi (Fig. 1C). For the proteomic experiment, almost 20% of SMZ (146 µM) was dissipated in 5 h pi and complete SMZ degradation observed at 24 h pi (Fig. 1D). As measured in the proteomic experiments, the ADMP end-transformation product was stoichiometrically produced upon the SMZ degradation, reaching 34 ± 2 (Fig. 1B) and 778 ± 23 µM (Fig. 1D) at 24 h pi for low and high SMZ concentrations, respectively. As expected, the strong ability of the *Microbacterium* sp. C448 strain to degrade SMZ is in accordance with literature, other *Microbacterium* strains also having the capacity to degrade sulphonamides (Tappe *et al.* 2013; Birkigt *et al.* 2015; Hirth *et al.* 2016; Ricken *et al.* 2017; Martin-Laurent *et al.* 2019).

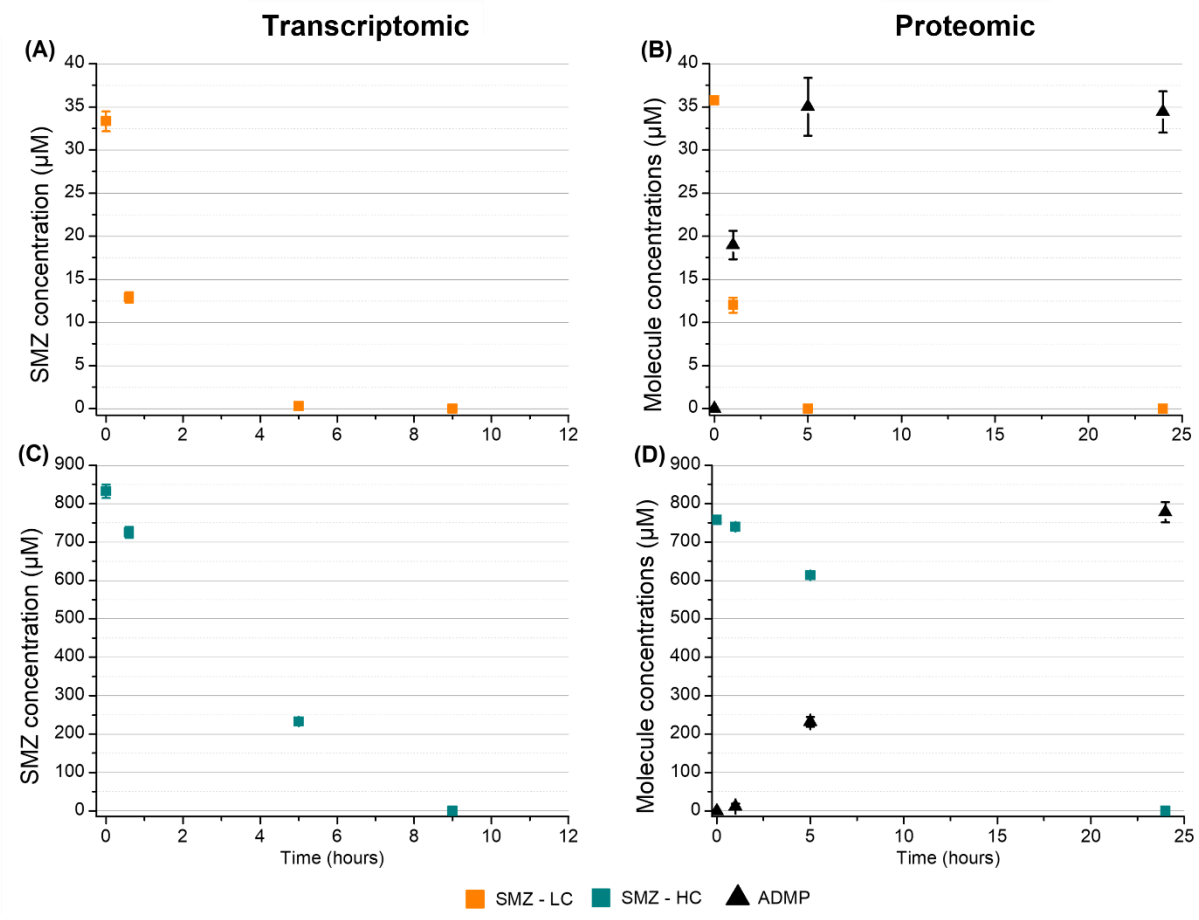

277

278 **Figure. 1. The degradation of SMZ by *Microbacterium* sp. C448.** The SMZ degradation (squares) and
279 the end-product ADMP production (▲) were quantified by HPLC in the *Microbacterium* sp. C448
280 cultures treated with the low (LC, 33 µM, ■) or the high (HC, 832 µM, ■) concentrations of SMZ, in
281 the transcriptomic (**A**, **C**) and in the proteomic experiments (**B**, **D**). The values are mean ± SD (n = 4).
282

283 **Sad responses to the SMZ biodegradation in *Microbacterium* sp. C448**

284 In the absence of SMZ (control), *sadABC* transcripts (Fig. 2A, 2C, and 2E) and the three Sad proteins,
285 found in the cytosolic fraction, were expressed or produced at baseline levels at the beginning of the
286 experiment (T0) (3.24 ± 0.06 AU of proteins in mean, Fig. 2B, 2D and 2F).

287 In the LC condition, as compared to the control, *sadB* (ORF 2028) and SadB (UniProt number W0Z833)
288 showed no significant difference in abundance throughout the incubation (Fig. 2C and D). In contrast,
289 the *sadA* (ORF 2030) and *sadC* (ORF 2026) transcripts increased significantly at 0.6 h pi by a factor of
290 1.8 and 1.9-fold, respectively (Fig. 2A and 2E, Table S1). Likewise, the abundance of SadA (W0Z5L8)
291 and SadC (W0Z7H5) protein increased by 1.5-fold at 1 h pi with SMZ (p = 0.011 and 0.002, respectively)

(Fig. 2B and 2F, Table S2). From 5 h pi, the abundances of the *sadA* and *sadC* transcripts were the same as the control. However, the abundances of SadA and SadC proteins were still increased at 5 h pi by 1.8 and 1.5-fold, respectively (p = 0.001 and 0.010). At 24 h pi, the abundance of the SadA protein remained increased by 1.5-fold (p = 0.009) while SadC proteins returned to the basal state (Fig. 2B and 2F). This slight difference observed between the transcriptomic and proteomic responses might be explained by the fact that the bacterial transcriptome responded more rapidly than the proteome to such an environmental change (Bathke *et al.* 2019).

In the HC condition, *sadB* transcript abundance was not changed (Fig. 2C), but the SadB protein abundance increased by 1.6-fold (p = 0.044) at 5 h pi (Fig. 2D). The abundances of *sadA* and *sadC* transcripts increased by 1.5 and 2.2-fold, respectively, at 0.6 h pi and by 3.1 and 2.6-fold, respectively, at 5 h pi (Fig. 2A and 2E, Table S1). At 9 h pi, these transcripts did not differ from the control. SadA protein abundance increased by 2.5-fold at 5h pi (p < 0.001) and last until the end of experiment (2.6-fold at 24 h pi, p < 0.001) (Fig. 2B). SadC protein abundance was increased all along the experiment by in mean 1.8-fold (p < 0.001) (Fig. 2F and Table S2). Therefore, while the *sadA* and *sadC* transcript production was transient, decreasing when the concentration of SMZ decreased in the medium, the SadA and SadC proteins persisted.

Overall, SadA and SadC proteins were found to be produced *in cellulo* by *Microbacterium* sp. C448 concomitantly to SMZ degradation and then continue to accumulate even after complete dissipation of the antibiotic. Moreover, their production depended on the initial exposure concentration to SMZ, suggesting their possible involvement in SMZ biodegradation, as observed before with purified enzymes (Kim *et al.* 2019b).

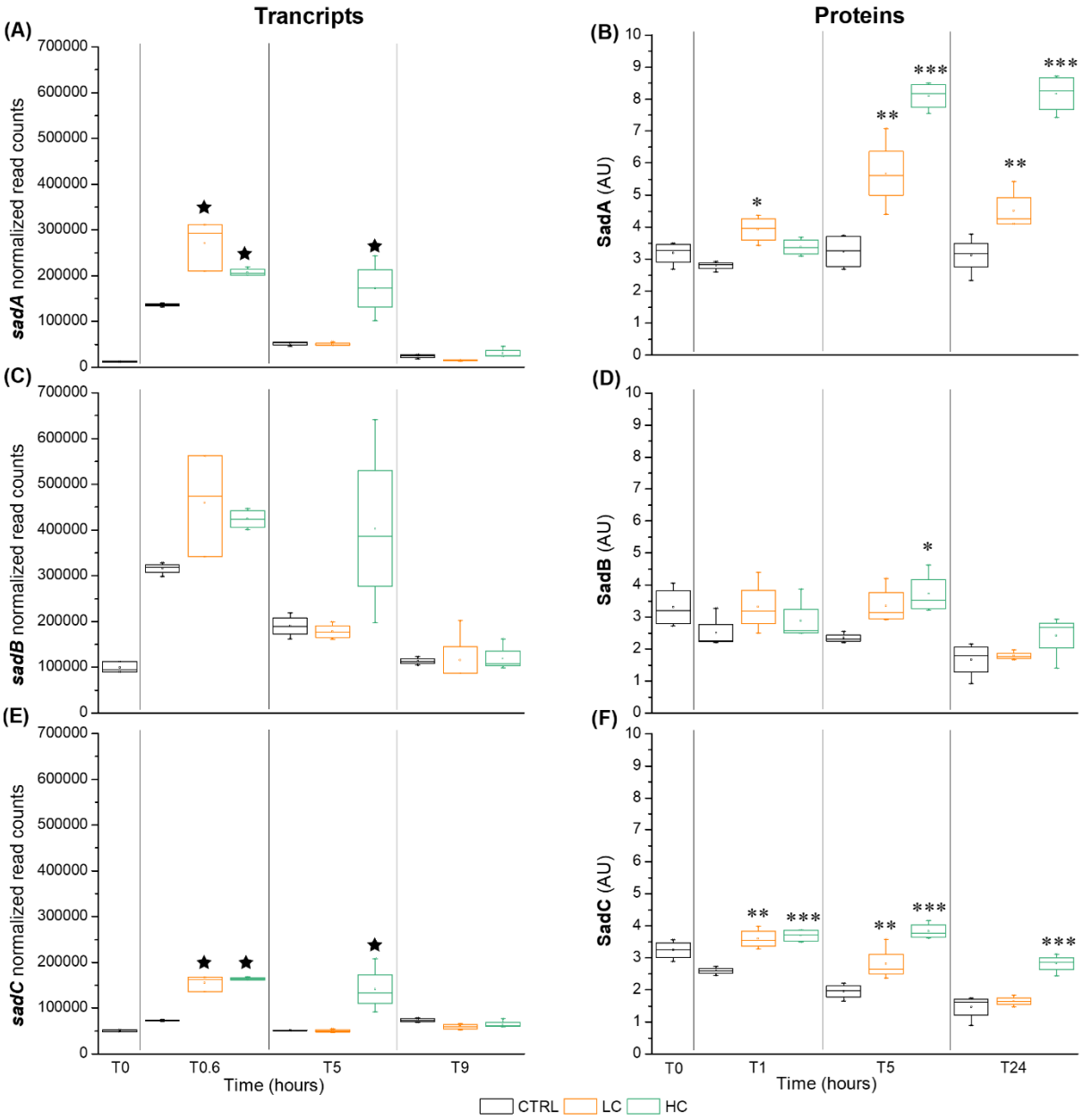

Figure. 2. Effect of the SMZ concentration on the abundance of *sad* transcripts and Sad proteins. The abundances of *sadA* (**A**), *sadB* (**C**) and *sadC* (**E**) transcripts and of the corresponding proteins (**B**, **D** and **F**) were reported, in the absence of SMZ (CTRL, ☐) and after exposure of *Microbacterium* sp. C448 to a low (LC, ☐) and a high (HC, ☐) concentration of SMZ at the different sampling times. Stars and asterisks represent the significant differences of transcripts (★: $p < 0.001$) and protein abundances (*: $p \leq 0.05$, **: $p \leq 0.01$ and ***: $p \leq 0.001$, see Table S1 for details) compared with the control for the same considered time.

DHPS gene expression and protein production

Numerous studies report the widespread occurrence of *sul1* and *sul2* genes coding for DHPS variants insensitive to SMZ in antibiotic contaminated environments as substitute of SMZ sensitive DHPS coded

326 by *folP* (*e.g.* Byrne-Bailey *et al.* 2009; Duan *et al.* 2019; Sardar *et al.* 2021). *Microbacterium* sp. C448
327 harbouring the *folP* and only *sul1* genes (Martin-Laurent *et al.* 2014) like other sulphonamide-
328 degrading Micrococcales (Kim *et al.* 2019b), their regulations were studied in presence of SMZ. The
329 *folP* transcript (ORF 1952) abundance was at least 7-fold lower than that of *sul1* (ORF 2696) for each
330 condition tested here (Fig. 3A and 3B). This trend was even more marked for the abundance of FolP
331 proteins (W0Z6Y9) detected in the cytosolic fraction which was 100-fold lower than that of Sul1
332 (W0Z673) all along the experiment (Fig. 3C and 3D). During the first five hours of incubation, the
333 abundances of *folP* and *sul1* transcripts were not affected by SMZ neither at LC nor HC. However, at
334 9h pi, the abundance of *folP* transcripts increased by 4.1- and 4.5-fold while the s*ul1* transcripts
335 decreased by 2.1 and 3.4-fold in LC and HC conditions, respectively (Table S1). Nevertheless, given the
336 fact that these modifications in the abundances of *folP* and of s*ul1* transcripts were observed only at a
337 time point where no more SMZ remained in the medium, one can hypothesise that these modifications
338 were not directly related to SMZ resistance or the metabolite ADMP which was previously shown not
339 to affect the *sul1* gene (Wu *et al.* 2022). The abundance of the FolP and Sul1 proteins was not affected
340 by SMZ either at LC nor at HC, whatever the sampling time, suggesting that the constitutive expression
341 of *sul1* allows a basal production enough to resist sulphonamide antibiotics (Fig. 3C and 3D, Table S2).
342

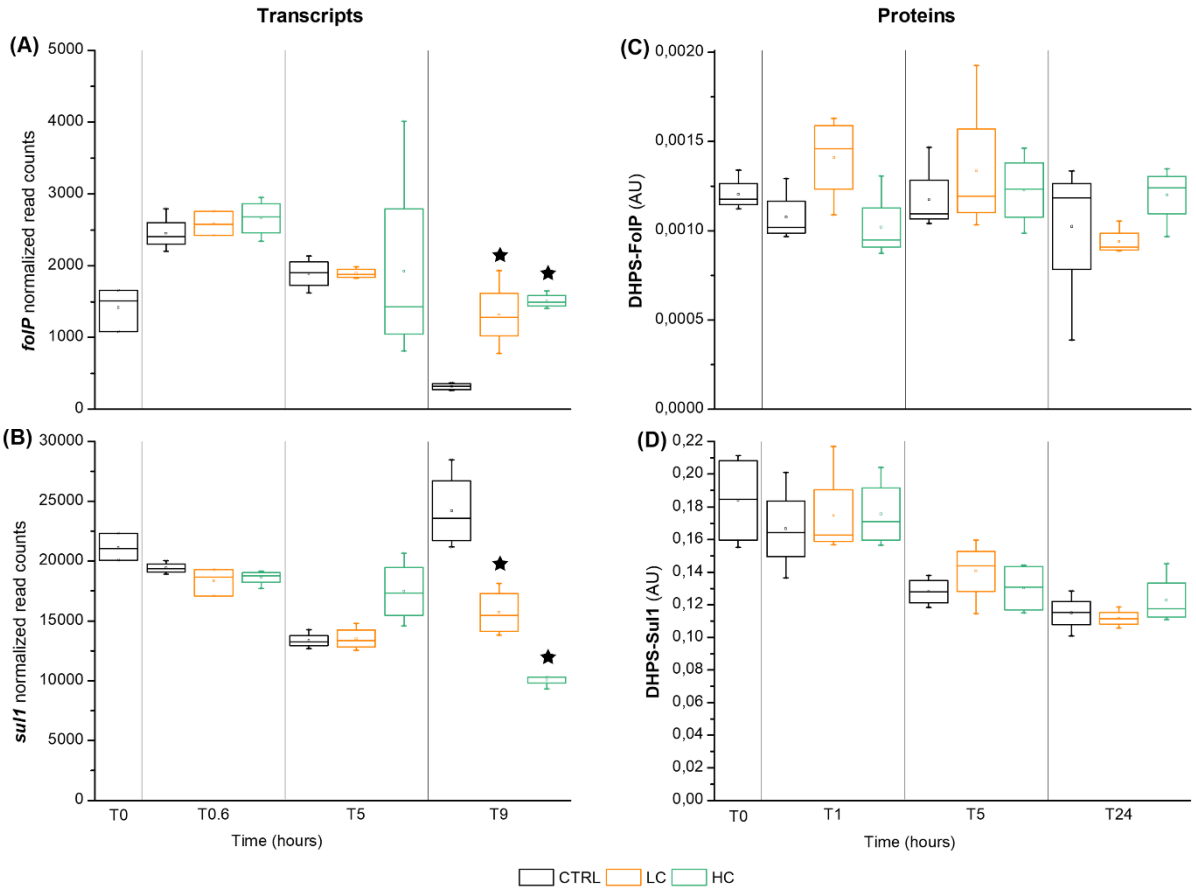

Figure 3. Effect of the SMZ concentration on the abundance of *folP* and *sul1* transcripts and FolP and Sul1 proteins. The abundance of *folP* (**A**) and *sul1* (**B**) transcripts were determined and the abundances of their corresponding proteins FolP (**C**) and Sul1 (**D**) were quantified in the presence of a low (LC, ☐) or a high (HC, ☐) SMZ concentration and compared with control (CTRL, ☐) for each sampling time (See Table S1). Stars represent the significant differences of transcript abundances compared with the control for the same considered time ($p < 0.001$).

Search for other genes/proteins potentially involved in the SMZ resistance

To further investigate the response of *Microbacterium* sp. C448 to SMZ exposure, other potential markers of resistance were explored such as those involved in stress response (Dorrian *et al.* 2011; Kim *et al.* 2017). Those showing a significant response were mainly overexpressed during the SMZ degradation phase and include chaperones, translation regulation, and DNA replication and repair factors (Table S3). Only one gene/protein (ORF 2019/W0Z991) was jointly evidenced by transcriptomic and proteomic data in the cytosolic fraction both in the LC and HC conditions (Table 1), and could have a preponderant role in the SMZ degradation process. The abundance of the RidA (Reactive

intermediate deaminase A) protein family coding gene transcript was increased by 2.3-fold in LC condition at 0.6 h pi and by 2.7- and 3.0-fold at 0.6 and 5 h pi, respectively, in HC condition. It was accompanied by a 2.3-fold increase of the RidA protein abundance at 5 h pi (p = 0.013). From 5 h pi, the abundances of the RidA coding gene transcript and its protein were not significantly different from the control. The RidA protein is a putative translation initiation inhibitor of the Rid family (formerly known as YjgF/YER057c/UK114). It leads to an enamine/imine deamination on intermediary metabolites produced during amino acid catabolism and converts them into keto acids, avoiding their accumulation and a metabolic perturbation of the cells (Flynn and Downs 2013; Ernst *et al.* 2014; Irons *et al.* 2020). Moreover, the Rid enzyme family was also described as having the capacity to degrade aromatic compounds, such as 2-aminophenol (Irons *et al.* 2020). The RidA protein family was also suggested to be involved in deamination of 4-aminophenol (4AP) (Rios-Miguel *et al.* 2022), an intermediate in the metabolism of sulphonamides by *Microbacterium* sp. C448. The hypothetical degradation of 4AP by RidA could also explain the low expression/production of SadB in our experiment, due to removal of its substrate (Fig. 2 and S1).

Except the stress response, the membrane-based efflux pumps are well known to be another resistance mechanism of bacteria to various antibiotics (Lubelski *et al.* 2007; Handzlik *et al.* 2013; Kumar and Patial 2016; Munita and Arias 2016; Schindler and Kaatz 2016; Greene *et al.* 2018; Reygaert 2018). Thus, although the sulphonamides are considered to passively pass through the cellular membrane, and that an uptake through unspecific transporters is not entirely excluded (Zarfl *et al.* 2007), the possible involvement of efflux pumps in the resistance of *Microbacterium* sp. C448 to SMZ exposure is unknown. Recently, the increase in the expression/production of ABC transporters was reported in *Escherichia coli* over-expressing *sul1* and *sul2*, suggesting the involvement of transporters in the bacterial resistance to sulphonamides (Zhou *et al.* 2021). In the present study, the exposure of *Microbacterium* sp. C448 to SMZ led to the modulation of 17 transporters in the cell envelope fraction, mainly related to the ABC transporter family. Under LC conditions, there were differences in the abundance of only a few transcripts and proteins (Table 1). At 9 h pi the abundance of one transporter

transcript was decreased (ORF 712: X 2.9) and another one was increased (ORF 327: X 2.3), but the abundances of the corresponding two proteins were not modified. However, the abundance of other transporter proteins was increased by 2.3-fold at 1 h pi (W0ZBZ8, $p = 0.018$) or decreased by 6.9-fold at 1 h pi (W0Z6W7, $p = 0.032$) and by 4.1-fold at 5 h pi (W0ZB95, $p = 0.041$). Exposure to antibiotics can cause up- or down-regulation of efflux pumps (Hemmerlin *et al.* 2014).

Under HC conditions, much more changes in gene expressions were recorded. At 0.6 h pi, the abundances of five transporter transcripts involved in sulphur, sugar or acetate metabolism were decreased by 2.0 to 2.9-fold while the abundance of one transporter transcript was increased by 2.4-fold (ORF 2808). From 5 h pi, the abundance of these transcripts was not affected by SMZ exposure except that of ORF 3047 which remained decreased by 2.6-fold. In addition, the abundance of three other ABC transporter transcripts probably belonging to glycine betaine transport systems were increased by 2.0 or 2.1-fold only at 5 h pi. Finally, the abundance of ORF 327 transcript was decreased by 2.3-fold at 5 h pi and 2.6-fold overexpressed at 9 h pi. The abundance of one putative ABC transporter protein (W0Z5S8) was decreased by 2.2-fold ($p = 0.013$) at 5 h pi and that of two others W0Z4F3 and W0ZDD8 were increased by 2.2 ($p = 0.024$) and 2.5-fold ($p = 0.032$) at 24 h pi, respectively (Table 1).

The combination of transcriptomic and proteomic analysis showed that the high abundance of one transcript (ORF 721) in particular was congruent with that of its related protein (W0Z8D9) in both LC and HC conditions (Table 1). It corresponds to a putative sulphate exporter family. Indeed, the abundance of this transcript was increased in LC conditions by 3-fold at 0.6 h pi and in HC conditions by 3.8-, 13.4- and 74.8-fold at 0.6, 5 and 9 h pi, respectively. Concomitantly, the abundance of the corresponding protein was increased in response to SMZ exposure in HC condition (by 5.4- and 75.8-fold at 5 and 24 h pi, respectively ($p < 0.001$)) (Table 1). This observation suggests that this efflux pump could be involved in the export of the sulphate residues, resulting from SMZ transformation, such as sulphurous acid H_2SO_3, or sulphuric acid H_2SO_4 (Macris and Markakis 1974; Kim *et al.* 2019b; Yu *et al.* 2020). We hypothesize that the up-regulation and -production of a sulphate efflux pump in

411 *Microbacterium* sp. C448 is associated with the removal of sulphur compounds produced by SMZ
412 metabolism that otherwise would reach toxic intracellular concentrations.

413 **Table 1. Genes and proteins potentially involved in *Microbacterium* sp. C448 resistance to SMZ.** The
414 nano-LC-MS/MS identified proteins harbouring a significant difference and with a minimum ± 2.0-fold
415 change between treated and control conditions are shown. A "/" indicates no differential expression.
416 Not detected indicates the protein abundance was below the detection threshold of the nano-LC-
417 MS/MS; LC and HC: low and high concentrations in SMZ; CTRL: control.

Category	Type	Domain	ORF	Gene name	UniProt code	Characteristics	LC						HC				
							Transcriptomic			Proteomic			Transcriptomic				Protec
							0.6 h pi	5 h pi	9 h pi	1 h pi	5 h pi	24 h pi	0.6 h pi	5 h pi	9 h pi	1 h pi	5 h pi
Translation	RidA family protein		2019	-	W0Z991	Putative translation initiation inhibitor YjgF family	+ 2.3	/	/	/	/	/	+ 2.7	+ 3.0	/	/	+ 2.3
Putative sulphate exporter		Uncharacterized	721	-	W0Z8D9	Putative membrane protein YeiH	+ 3.0	/	/	/	/	/	+ 3.8	+ 13.8	+ 74.8	/	+ 5.4
ABC	-	SBP	712	-	W0Z5S8	Putative protein	/	/	- 2.9	/	/	/	/	/	- 2.6	/	- 2.2
			2176	-	W0ZB95	NMT1/THI5 like domain protein	/	/	/	/	- 4.1	/	/	/	/	/	/
			1014	-	W0Z9I1	Nitrate/sulfonate/bicarbonate transporter	/	/	/	Not detected			- 2.2	/	/		Not det
		Uncharacterized	1016	-	W0ZA46	Alkanesulfonate transport system permease protein	/	/	/	Not detected			- 2.3	/	/		Not det
		SBP	2228	*opuAC*	W0ZAE6	Proline/glycine betaine transport systems	/	/	/	Not detected			/	+ 2.1	/		Not det
			2230	*proV*	W0ZBF3	Glycine betaine transporter	/	/	/	/	/	/	/	+ 2.0	/	/	/
		Uncharacterized	2229	*opuAB*	W0ZCJ6	Glycine betaine transport system permease protein OpuAB	/	/	/	/	/	/	/	+ 2.0	/	/	/
		TMD	585	-	W0Z4F3	Transport permease protein	/	/	/	/	/	/	/	/	/	/	/
			244	*ssuC*	W0ZDD8	Alkanesulfonate transporter subunit membrane component	/	/	/	/	/	/	/	/	/	/	/
		NBD	265	*livF*	W0ZBZ8	Leucine/isoleucine/valine transporter	/	/	/	+ 2.3	/	/	/	/	/	/	/
	ATP-binding protein	Uncharacterized	327	*drrA*	W0ZCT4	Daunorubicin/doxorubicin resistance	/	/	+ 2.3	/	/	/	/	- 2.3	+ 2.6	/	/
	BMP	SBP	533	-	W0Z6W7	Uncharacterized protein	/	/	/	- 6.9	/	/	/	/	/	/	/
	Monosaccharide	SBP	2159	-	W0ZEB5	Cluster maltose/g3p/polyamine/iron - extracellular solute-binding protein	/	/	/	/	/	/	- 2.1	/	/	/	/
			2446	-	W0Z4P9	Cluster ribose/xylose/arabinose/galactose	/	/	/	Not detected			- 2.9	/	/		Not det
APC	SSS	Uncharacterized	3047	*actP*	W0ZC79	Cation/acetate symporter	/	/	/	/	/	/	- 2.0	- 2.6	/	/	/
MSF	-	Uncharacterized	2808	-	W0ZCN7	Permease of MSF-type transporter	/	/	/	Not detected			+ 2.4	/	/		Not det

Conclusions

In agreement with *in vitro* findings, the congruence of our transcriptomic and proteomic results reveals for the first time the involvement, *in cellulo*, of Sad pathway in the SMZ degradation in *Microbacterium* sp. C448. Contrary to our initial hypothesis whereby *sul1* would be required to permit biodegradation of the drug at therapeutic concentration, we found that the basal expression of *sul1* conferred a natural resistance to *Microbacterium* sp. C448, enough to cope with SMZ. Furthermore, this study has revealed for the first time proteins that may be involved in the metabolism of the key sulphonamide intermediate 4-aminophenol, and the export of inorganic sulphur species that may be toxic if they accumulate in the cell. These conclusions need to be verified and confirmed experimentally. This study contributes to a better understanding of the response of the SMZ-degrading *Microbacterium* sp. C448 strain to sulphonamide exposure and provided new insights into SMZ detoxification process.

Acknowledgments

This work was supported by the Agence Nationale de la Recherche (ANTIBIOTOX project; grant number ANR-17-CE34-0003).

References

Amezaga MR, Davidson I, McLaggan D *et al.* The role of peptide metabolism in the growth of *Listeria monocytogenes* ATCC 23074 at high osmolarity. *Microbiology* 1995;**141**:41–9.

Annergren M, Larsson CA. MOOSE2—A toolbox for least-costly application-oriented input design. *SoftwareX* 2016;**5**:96–100.

Anses. *Surveillance Des Ventes de Médicaments Vétérinaires Contenant Des Antibiotiques En France En 2021. Rapport Annuel*., 2022.

Bathke J, Konzer A, Remes B *et al.* Comparative analyses of the variation of the transcriptome and

443 proteome of *Rhodobacter sphaeroides* throughout growth. *BMC Genomics* 2019;**20**:358.

444 Ben Y, Fu C, Hu M *et al.* Human health risk assessment of antibiotic resistance associated with antibiotic
445 residues in the environment: A review. *Environ Res* 2019;**169**:483–93.

446 Benjamini Y, Hochberg Y. Controlling the False Discovery Rate: A Practical and Powerful Approach to
447 Multiple Testing. *J R Stat Soc Ser B* 1995;**57**:289–300.

448 Birkigt J, Gilevska T, Ricken B *et al.* Carbon stable isotope fractionation of sulfamethoxazole during
449 biodegradation by *Microbacterium* sp. strain BR1 and upon direct photolysis. *Environ Sci Technol*
450 2015;**49**:6029–36.

451 van Boeckel TP, Glennon EE, Chen D *et al.* Reducing antimicrobial use in food animals. *Science (80-)*
452 2017;**357**:1350–2.

453 Bouju H, Ricken B, Beffa T *et al.* Isolation of bacterial strains capable of sulfamethoxazole
454 mineralization from an acclimated membrane bioreactor. *Appl Environ Microbiol* 2012;**78**:277–
455 9.

456 Byrne-Bailey KG, Gaze WH, Kay P *et al.* Prevalence of sulfonamide resistance genes in bacterial isolates
457 from manured agricultural soils and pig slurry in the United Kingdom. *Antimicrob Agents*
458 *Chemother* 2009;**53**:696–702.

459 Cao L, Zhang J, Zhao R *et al.* Genomic characterization, kinetics, and pathways of sulfamethazine
460 biodegradation by *Paenarthrobacter* sp. A01. *Environ Int* 2019;**131**:104961.

461 Capasso C, Supuran CT. Sulfa and trimethoprim-like drugs – antimetabolites acting as carbonic
462 anhydrase, dihydropteroate synthase and dihydrofolate reductase inhibitors. *J Enzyme Inhib Med*
463 *Chem* 2014;**29**:379–87.

464 Chen J, Jiang X, Tong T *et al.* Sulfadiazine degradation in soils: Dynamics, functional gene, antibiotic
465 resistance genes and microbial community. *Sci Total Environ* 2019;**691**:1072–81.

Chen J, Xie S. Overview of sulfonamide biodegradation and the relevant pathways and microorganisms. *Sci Total Environ* 2018;**640**–**641**:1465–77.

Connor EE. Sulfonamide antibiotics. *Prim Care Update Ob Gyns* 1998;**5**:32–5.

Cycoń M, Mrozik A, Piotrowska-Seget Z. Antibiotics in the soil environment—degradation and their impact on microbial activity and diversity. *Front Microbiol* 2019;**10**, DOI: 10.3389/fmicb.2019.00338.

Deng Y, Li B, Zhang T. Bacteria That Make a Meal of Sulfonamide Antibiotics: Blind Spots and Emerging Opportunities. *Environ Sci Technol* 2018;**52**:3854–68.

Dorrian JM, Briggs DA, Ridley ML *et al.* Induction of a stress response in *Lactococcus lactis* is associated with a resistance to ribosomally active antibiotics. *FEBS J* 2011;**278**:4015–24.

Duan M, Gu J, Wang X *et al.* Factors that affect the occurrence and distribution of antibiotic resistance genes in soils from livestock and poultry farms. *Ecotoxicol Environ Saf* 2019;**180**:114–22.

Duan W, Cui H, Jia X *et al.* Occurrence and ecotoxicity of sulfonamides in the aquatic environment: A review. *Sci Total Environ* 2022;**820**:153178.

Ernst DC, Lambrecht JA, Schomer RA *et al.* Endogenous synthesis of 2-aminoacrylate contributes to cysteine sensitivity in *Salmonella enterica*. *J Bacteriol* 2014;**196**:3335–42.

Esbelin J, Santos T, Ribière C *et al.* Comparison of three methods for cell surface proteome extraction of *Listeria monocytogenes* biofilms. *Omi A J Integr Biol* 2018;**22**:779–87.

Feng L, Casas ME, Ottosen LDM *et al.* Removal of antibiotics during the anaerobic digestion of pig manure. *Sci Total Environ* 2017;**603**–**604**:219–25.

Flynn JM, Downs DM. In the absence of RidA, endogenous 2-aminoacrylate inactivates alanine racemases by modifying the pyridoxal 5'-phosphate cofactor. *J Bacteriol* 2013;**195**:3603–9.

Greene NP, Kaplan E, Crow A *et al.* Antibiotic resistance mediated by the MacB ABC transporter family:

A structural and functional perspective. *Front Microbiol* 2018;**9**:950.

Handzlik J, Matys A, Kieć-Kononowicz K. Recent Advances in Multi-Drug Resistance (MDR) Efflux Pump Inhibitors of Gram-Positive Bacteria *S. aureus*. *Antibiot (Basel, Switzerland)* 2013;**2**:28–45.

Hemmerlin A, Tritsch D, Hammann P *et al.* Profiling of defense responses in *Escherichia coli* treated with fosmidomycin. *Biochimie* 2014;**99**:54–62.

Hirth N, Topp E, Dörfler U *et al.* An effective bioremediation approach for enhanced microbial degradation of the veterinary antibiotic sulfamethazine in an agricultural soil. *Chem Biol Technol Agric* 2016;**3**:1–11.

Hu J, Li X, Liu F *et al.* Comparison of chemical and biological degradation of sulfonamides: Solving the mystery of sulfonamide transformation. *J Hazard Mater* 2022;**424**:127661.

Irons JL, Hodge-Hanson K, Downs DM. RidA Proteins Protect against Metabolic Damage by Reactive Intermediates. *Microb Mol Biol Rev* 2020;**84**:e00024-20.

Kim CK, Milheiriço C, De Lencastre H *et al.* Antibiotic resistance as a stress response: Recovery of high-level oxacillin resistance in methicillin-resistant *Staphylococcus aureus* "auxiliary" (fem) mutants by induction of the stringent stress response. *Antimicrob Agents Chemother* 2017;**61**:e00313-17.

Kim D, Paggi JM, Park C *et al.* Graph-based genome alignment and genotyping with HISAT2 and HISAT-genotype. *Nat Biotechnol* 2019a;**37**:907–15.

Kim DW, Thawng CN, Lee K *et al.* A novel sulfonamide resistance mechanism by two-component flavin-dependent monooxygenase system in sulfonamide-degrading actinobacteria. *Environ Int* 2019b;**127**:206–15.

Kumar R, Patial SJP. A Review on Efflux Pump Inhibitors of Gram-Positive and Gram-Negative Bacteria from Plant Sources. *Int J Curr Microbiol Appl Sci* 2016;**5**:837–55.

Liao Y, Smyth GK, Shi W. featureCounts: an efficient general purpose program for assigning sequence

512 reads to genomic features. *Bioinformatics* 2014;**30**:923–30.

513 Love MI, Huber W, Anders S. Moderated estimation of fold change and dispersion for RNA-seq data
514 with DESeq2. *Genome Biol* 2014;**15**:1–21.

515 Lubelski J, Konings WN, Driessen AJM. Distribution and Physiology of ABC-Type Transporters
516 Contributing to Multidrug Resistance in Bacteria. *Microbiol Mol Biol Rev* 2007;**71**:463–76.

517 Macris BJ, Markakis P. Transport and Toxicity of Sulphur Dioxide in *Saccharomyces cerevisiae* var
518 *ellipsoideus*. *J Sci Food Agric* 1974;**25**:21–9.

519 Martin-Laurent F, Marti R, Waglechner N *et al.* Draft genome sequence of the sulfonamide antibiotic-
520 degrading *Microbacterium* sp. strain C448. *Genome Announc* 2014;**2**:e01113-13.

521 Martin-Laurent F, Topp E, Billet L *et al.* Environmental risk assessment of antibiotics in agroecosystems:
522 ecotoxicological effects on aquatic microbial communities and dissemination of antimicrobial
523 resistances and antibiotic biodegradation potential along the soil-water continuum. *Environ Sci*
524 *Pollut Res* 2019;**26**:18930–7.

525 Martin M. Cutadapt removes adapter sequences from high-throughput sequencing reads.
526 *EMBnet.journal* 2011;**17**:10–2.

527 Mulla SI, Bagewadi ZK, Faniband B *et al.* Various strategies applied for the removal of emerging
528 micropollutant sulfamethazine: a systematic review. *Environ Sci Pollut Res* 2021, DOI:
529 10.1007/s11356-021-14259-w.

530 Munita JM, Arias CA. Mechanisms of Antibiotic Resistance. *Microbiol Spectr* 2016;**4**, DOI:
531 10.1128/MICROBIOLSPEC.VMBF-0016-2015.

532 National Academy of Pharmacy. *Medicinal Products and Environment*., 2019.

533 Nunes OC, Manaia CM, Kolvenbach BA *et al.* Living with sulfonamides: a diverse range of mechanisms
534 observed in bacteria. *Appl Microbiol Biotechnol* 2020;**104**:10389–408.

535 Perreten V, Boerlin P. A new sulfonamide resistance gene (*sul3*) in *Escherichia coli* is widespread in the
536 pig population of Switzerland. *Antimicrob Agents Chemother* 2003;**47**:1169–72.

537 Perri R, Kolvenbach BA, Corvini PFX. Subsistence and complexity of antimicrobial resistance on a
538 community-wide level. *Environ Microbiol* 2020;**22**:2463–8.

539 Reygaert WC. An overview of the antimicrobial resistance mechanisms of bacteria. *AIMS Microbiol*
540 2018;**4**:482–501.

541 Ricken B, Kolvenbach BA, Bergesch C *et al.* FMNH2-dependent monooxygenases initiate catabolism of
542 sulfonamides in *Microbacterium* sp. strain BR1 subsisting on sulfonamide antibiotics. *Sci Rep*
543 2017;**7**:1–11.

544 Rios-Miguel AB, Smith GJ, Cremers G *et al.* Microbial paracetamol degradation involves a high diversity
545 of novel amidase enzyme candidates. *Water Res X* 2022;**16**:100152.

546 Santos T, Hébraud M. Extraction and preparation of *Listeria monocytogenes* subproteomes for mass
547 spectrometry analysis. *Methods Mol Biol* 2021;**2220**:137–53.

548 Sardar MF, Zhu C, Geng B *et al.* Enhanced control of sulfonamide resistance genes and host bacteria
549 during thermophilic aerobic composting of cow manure. *Environ Pollut* 2021;**275**:116587.

550 Schindler BD, Kaatz GW. Multidrug efflux pumps of Gram-positive bacteria. *Drug Resist Updat*
551 2016;**27**:1–13.

552 Sköld O. Sulfonamide resistance: mechanisms and trends. *Drug Resist Updat* 2000;**3**:155–60.

553 Spielmeyer A. Occurrence and fate of antibiotics in manure during manure treatments: A short review.
554 *Sustain Chem Pharm* 2018;**9**:76–86.

555 Spielmeyer A, Höper H, Hamscher G. Long-term monitoring of sulfonamide leaching from manure
556 amended soil into groundwater. *Chemosphere* 2017;**177**:232–8.

557 Tappe W, Herbst M, Hofmann D *et al.* Degradation of sulfadiazine by *Microbacterium lacus* strain

SDZm4, isolated from lysimeters previously manured with slurry from sulfadiazine-medicated pigs. *Appl Environ Microbiol* 2013;**79**:2572–7.

Topp E, Chapman R, Devers-Lamrani M *et al.* Accelerated biodegradation of veterinary antibiotics in agricultural soil following long-term exposure, and isolation of a sulfamethazine-degrading *Microbacterium* sp. *J Environ Qual* 2013;**42**:173–8.

Wu J, Zhang Y, Huang M *et al.* Sulfonamide antibiotics alter gaseous nitrogen emissions in the soil-plant system: A mesocosm experiment and meta-analysis. *Sci Total Environ* 2022;**828**:154230.

Yu L, Wang Y, Su X *et al.* Biodiversity, isolation and genome analysis of sulfamethazine-degrading bacteria using high-throughput analysis. *Bioprocess Biosyst Eng* 2020;**43**:1521–31.

Zarfl C, Matthies M, Klasmeier J. A mechanistical model for the uptake of sulfonamides by bacteria. *Chemosphere* 2007;**70**:753–60.

Zhou Y, Fang J, Davood Z *et al.* Fitness cost and compensation mechanism of sulfonamide resistance genes (*sul1*, *sul2*, and *sul3*) in *Escherichia coli*. *Environ Microbiol* 2021;**23**:7538–49.

Supplemental data

Fig. S1. Proposed SMZ degradation pathway catalysed by Sad proteins in *Microbacterium* sp. C448. SadA and SadB: monooxygenases; SadC: flavine reductase (according to Ricken *et al.* 2017 and Kim *et al.* 2019b).

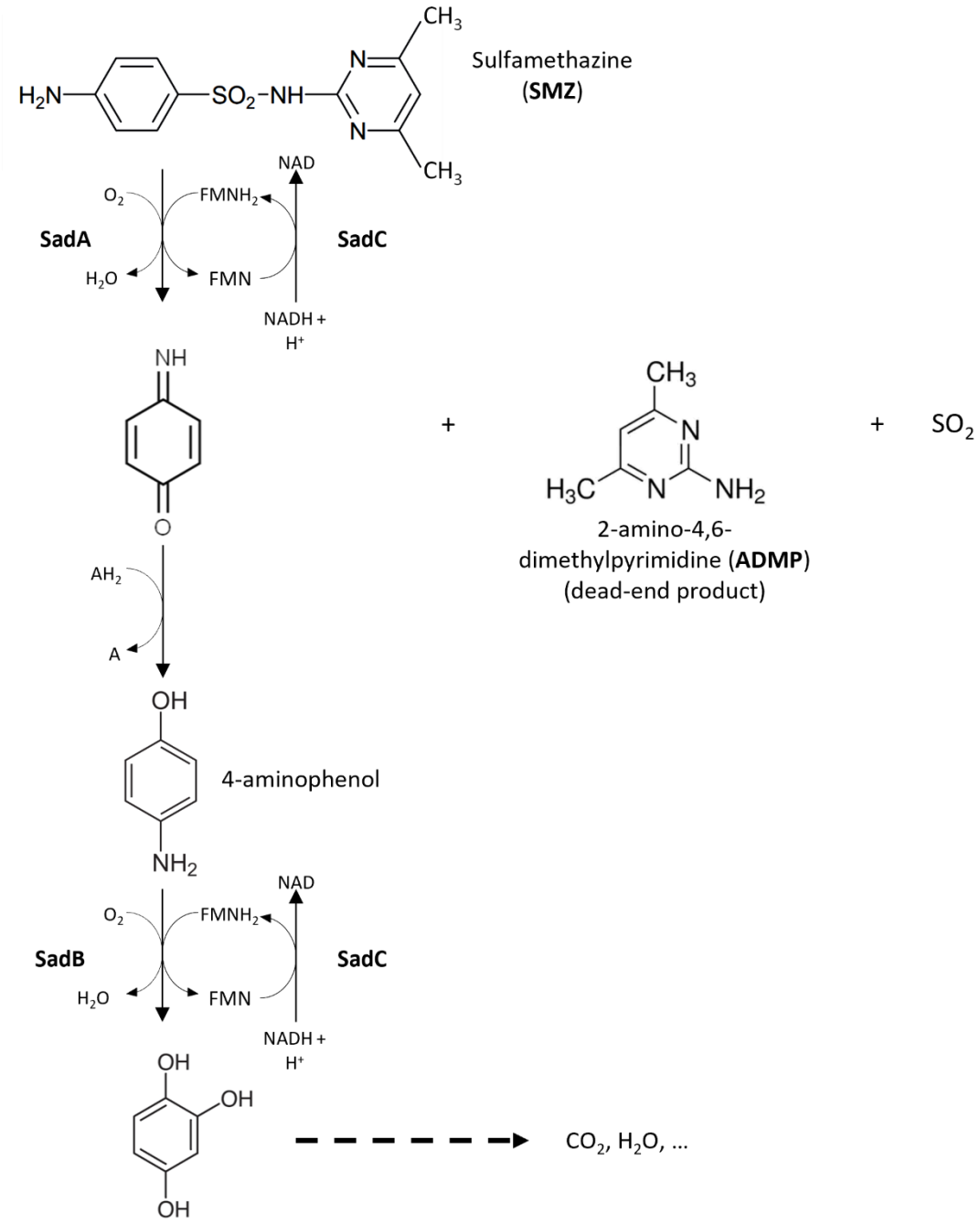

Table S1. Modification of the abundance of *sadABC*, *folP* and *sul1* transcripts obtained from DeSeq2 analysis. Any statistically significant difference of transcript abundance is expressed as fold-change as compared to control (n = 4, $p < 0.001$). CTRL: control; LC: low SMZ concentration; HC: high SMZ concentration; +: increase; -: decrease; NS: not significant.

586

587

588

Time (h)	Comparison	*sadA* ORF 2030	*sadB* ORF 2028	*sadC* ORF 2026	*folP* ORF 1952	*sul1* ORF 2696
0.6	LC *vs* CTRL	+1.8	NS	+1.9	NS	NS
	HC *vs* CTRL	+1.5	NS	+2.2	NS	NS
5	LC *vs* CTRL	NS	NS	NS	NS	NS
	HC *vs* CTRL	+3.1	NS	+2.6	NS	NS
9	LC *vs* CTRL	NS	NS	NS	+4.1	-2.1
	HC *vs* CTRL	NS	NS	NS	+4.5	-3.4

Table S2. Adjusted *p*-values obtained after the Dunn tests was applied on the abundance of Sad and DHPS proteins after exposure of *Microbacterium* sp. C448 to SMZ. CTRL: control; LC: low concentration; HC: high concentration; +: increase; -: decrease; =: no difference; NS: not significant. Bold characters: significant data.

Time (h)	Comparison	Sad A W0Z5L8		Sad B W0Z833		Sad C W0Z7H5		DHPS-*folP* W0Z6Y9		DHPS-*sul1* W0Z673	
		Fold-change	*p* value	Fold-change	*p* value	Fold-change	*p* value	Fold-change	*p* value	Fold-change	*p* value
1	LC *vs* CTRL	**+1.5**	**0.011**	+1.3	NS	**+1.5**	**0.002**	+1.3	NS	=1.0	NS
	HC *vs* CTRL	+1.2	NS	+1.2	NS	**+1.5**	**0.000**	-1.1	NS	+1.1	NS
5	LC *vs* CTRL	**+1.8**	**0.001**	+1.4	NS	**+1.5**	**0.010**	+1.1	NS	+1.1	NS
	HC *vs* CTRL	**+2.5**	**0.000**	**+1.6**	**0.044**	**+2.0**	**0.000**	=1.0	NS	=1.0	NS
24	LC *vs* CTRL	**+1.5**	**0.009**	+1.1	NS	+1.1	NS	-1.1	NS	=1.0	NS
	HC *vs* CTRL	**+2.6**	**0.000**	+1.4	NS	**+1.9**	**0.000**	+1.2	NS	+1.1	NS

Table S3. List of the stress markers modulated in *Microbacterium* sp. C448 exposed to SMZ. Any statistically significant modification of transcript abundance is expressed as fold change as compared to control ($p < 0.001$). The adjusted *p*-values of proteins are indicated in parentheses.

Category	Type	ORF	Gene name	UniProt code	Characteristics	LC						HC					
						Transcriptomic			Proteomic			Transcriptomic			Proteomic		
						0.6 h pi	5 h pi	9 h pi	1 h pi	5 h pi	24 h pi	0.6 h pi	5 h pi	9 h pi	1 h pi	5 h pi	24 h pi
Translation	RidA family protein	2019	-	W0Z991	Putative translation initiation inhibitor YjgF family	+ 2.3	/	/	/	/	/	+ 2.7	+ 3.0	/	/	+ 2.3 (p = 0.013)	/
	Initiation factor IF1	189	*infA*	W0Z9Z0	-	/	/	- 3.6	/	/	/	/	+ 2.2	- 6.4	/	/	/
	30S ribosomal protein S1	1506	*rpsA*	W0ZEG5	Cell division-ribosomal stress proteins cluster	/	/	/	/	/	/	/	+ 2.1	- 2.5	/	/	/
	Ribonuclease P protein component	2283	*rnpA*	W0ZBK8	Cell division subsystem	/	/	- 3.4	Not detected			/	+ 2.1	- 5.3	Not detected		
Chaperone	Foldase YidC	2285	*yidC*	W0ZD69	Membrane protein insertase	/	/	/	+ 2.0 (p = 0.005)	/	/	/	/	/	/	/	/
	Heat shock	2616	-	W0ZER6	18 kDa antigen 2, belongs to the HSP20 family	/	/	/	Not detected			+ 2.2	+ 2.3	/	Not detected		
		251	*groS*	W0ZAX2	10 kDa family GroES	/	/	/	/	/	/	/	+ 2.5	/	/	/	/
		2931	-	W0Z6T0	60 kDa family GroEL	/	/	/	Not detected				+ 2.4		Not detected		
	Cold shock	2938	-	W0Z7K5	Cold shock domain-containing protein	/	/	/	/	+ 2.0 (p = 0.032)	/	/	/	/	/	/	/
	Trigger factor	1439	*tig*	W0Z731	EC:5.2.1.8	/	/	/	/	- 2.6 (p = 0.024)	/	/	/	/	/	/	/
DNA replication & repair	Primosomal protein	1745	-	W0ZB93	TPR-repeat-containing protein	/	/	/	/	/	/	/	+ 2.5	/	/	/	/
	Single-stranded DNA-binding protein	2306	*ssb*	W0ZC46	RecFOR pathway	/	/	/	/	/	/	/	+ 2.4	/	/	/	/